

Nuclear Moments of Sc^{44} and $\text{Sc}^{44m}\dagger$

D. L. HARRIS AND J. D. MCCULLEN

Palmer Physical Laboratory, Princeton University, Princeton, New Jersey

(Received 16 May 1963)

The nuclear moments of Sc^{44} and Sc^{44m} have been measured using the atomic beam magnetic resonance method. The results are:

$$\begin{aligned} I=2, \quad |\mu| &= 2.56 \pm 0.03 \text{ nm}, \quad |Q| = 0.14 \pm 0.08 \text{ b}, \quad \text{with } \mu/Q > 0; \\ I=6, \quad |\mu| &= 3.96 \pm 0.15 \text{ nm}, \quad |Q| = 0.37 \pm 0.29 \text{ b}, \quad \text{with } \mu/Q < 0. \end{aligned}$$

Observations of multiple quantum transitions in the $I=2$ state give a value for g_J in the ${}^2D_{5/2}$ electronic state of 1.2008 ± 0.0003 if $\mu(I=2) > 0$, $g_J = 1.1997 \pm 0.0003$ if $\mu(I=2) < 0$. These results are discussed with emphasis on the pertinence of the odd-group model for odd-odd nuclei in this region of the periodic table.

I. INTRODUCTION

FOR the past several years this laboratory has studied the spins and moments of radioactive odd-odd nuclei in several regions of the periodic table. Emphasis has been placed on the interpretation of the measurements in terms of specific nuclear wave functions. For the most part, the nuclei which have been studied have proved consistent with some type of odd-group model,¹ in which neutron and proton configurations are treated separately, and in which the total spin I is just the net spin formed by coupling together the total proton and total neutron spins, I_p and I_n . If neutrons and protons are filling different shell-model levels, the assumptions of this model may be valid. Where the same level is being filled by both kinds of nucleon, however, it will probably break down, because the neutron-proton interaction will mix states of different I_p and I_n . An example of the breakdown might be expected in ${}_{25}\text{Mn}_{27}^{52}$, where neutrons and protons both fill the $f_{7/2}$ shell. Recent measurements² of the magnetic moments of Mn^{52} , however, have shown remarkable agreement with the simple model. To see if the agreement was a general result throughout the shell, we have investigated the moments of the two long-lived states of ${}_{21}\text{Sc}_{23}^{44}$, the particle conjugate of Mn^{52} . The spins of these levels have been previously reported.³

The measurements were performed using the atomic beam magnetic resonance technique. In the atomic beam apparatus, dipole transitions are induced by an rf field between magnetic sublevels of the hyperfine atomic levels, and the frequencies of the transitions are followed as a function of magnetic field. From these measurements the energy level spacings in the hyperfine structure (hfs) of the free atom can be determined. As in several previous investigations in this laboratory,⁴⁻⁶

the investigation was facilitated by the observation of multiple-quantum absorption transitions.

II. EXPERIMENT

The apparatus used in the experiments was the focusing atomic beam machine of Lemonick, Pipkin, and Hamilton.⁷ Subsequent modifications and some details of the machine operation have previously appeared in the literature.^{5,6} The apparatus consists of three magnets through which the atomic beam is passed. The first and last of these are six-pole magnets which focus atoms of a given sign of the atomic moment towards the axis of the machine, and deflect atoms of the opposite sign away from the axis out of the transmitted beam. The center "C" magnet is a homogeneous one; in its field is a loop powered by an rf signal generator. If the applied frequency is appropriate, transitions will be induced at the loop such that the sign of the atom's effective moment changes. The "unflopped" beam is collected and monitored by placing a small copper button on axis behind the last magnet. Those atoms which have been "flopped" at the loop are collected on a larger disk concentric to the button. These collectors are then removed from the machine through an airlock, and the collected activity counted with a scintillation counter.

The activity for this experiment was produced by the (p, pn) reaction on 99.8% pure Sc^{45} metal. Most of the activity for the study of the 4-h state was produced using the 18-MeV protons from the Princeton cyclotron. For the production of the 2.4-day state the metal was bombarded in the 86-in. cyclotron at Oak Ridge National Laboratory. The atomic beam was produced from a double walled tantalum oven heated to $\sim 1600^\circ\text{C}$ by electron bombardment.

The collecting surfaces were clean copper, scoured with steel wool to present a fresh surface, and rinsed in alcohol and acetone. The combination of source

[†] This work was supported by the U. S. Atomic Energy Commission and the Higgins Scientific Trust Fund.

¹ M. H. Brennan and A. M. Bernstein, *Phys. Rev.* **120**, 927 (1960); reference to earlier papers may be found in this reference.

² R. W. Bauer, Martin Deutsch, G. S. Mutchler, and D. G. Simons, *Phys. Rev.* **120**, 946 (1960).

³ D. L. Harris and J. D. McCullen, *Bull. Am. Phys. Soc.* **6**, 224 (1961).

⁴ R. L. Christensen, D. R. Hamilton, H. G. Bennowitz, J. B. Reynolds, and H. H. Stroke, *Phys. Rev.* **122**, 1361 (1961).

⁵ O. Ames, A. M. Bernstein, M. H. Brennan, and D. R. Hamilton, *Phys. Rev.* **123**, 1793 (1961).

⁶ J. C. Walker, *Phys. Rev.* **127**, 1739 (1962).

⁷ A. Lemonick, F. M. Pipkin, and D. R. Hamilton, *Rev. Sci. Instr.* **26**, 1112 (1955).

strength, oven temperature, and collecting efficiency was such to give counting rates of about 1000 counts/min on the monitor button for five minute exposures to the beam. This beam could be maintained for several hours. Ratios of the outer disk to monitor button counting rates (d/b) were of the order of 0.030 with no rf field present, and would rise as high as 0.100 on resonance.

The rf power necessary to induce transitions was supplied by a Rohde-Schwarz SMLR oscillator fed to the 10-turn solenoidal loop. The C -field intensity was monitored by measuring the transition frequency in stable K^{39} , using a separate low temperature oven and a hot wire detector which could be rotated into and out of the beam. The power fed to the solenoid was monitored with a pickup loop; the frequency, by a Hewlett-Packard 524-B cycle counter. Use of the solenoid enabled us to attain the high rf field necessary for the multiple-quantum studies.

III. HFS THEORY

The hfs energy of a free atom, which is due to the interaction of the nuclear moments with the field of the atomic electrons, may be described in terms of the electron spin J and the nuclear spin I by the Hamiltonian

$$H_{\text{hfs}} = hA(\mathbf{I} \cdot \mathbf{J}) + hB \left(\frac{3(\mathbf{I} \cdot \mathbf{J})^2 + \frac{3}{2}(\mathbf{I} \cdot \mathbf{J}) - I(I+1)J(J+1)}{2I(I-1)2J(J-1)} \right), \quad (1)$$

if octupole and higher-order interactions are neglected. In this equation, A and B are proportional to the nuclear moments μ_I and Q ;

$$A = -\frac{1}{h} \frac{\mu_I}{I} \left\langle \frac{H(0)}{J} \right\rangle, \quad (2)$$

$$B = -\frac{e}{h} Q_I \left\langle \frac{\partial E}{\partial z} \right\rangle.$$

$\langle H(0) \rangle$ is the magnetic field and $\langle \partial E / \partial z \rangle$ the electric field gradient at the nucleus produced by the atomic electrons, and μ_I and Q are the nuclear moments. The electron charge e is here taken as a negative number. This Hamiltonian is diagonal in the $(IJFM_F)$ representation, and the eigenvalues are simply expressed as linear equations in A and B .

When an external magnetic field H_E is applied, there is the further interaction,

$$H_{\text{mag}} = g_J \mu_0 (\mathbf{J} \cdot \mathbf{H}_E) + g_I' \mu_0 (\mathbf{I} \cdot \mathbf{H}_E), \quad (3)$$

which splits the magnetic sublevels of the hyperfine states (the eigenfunctions of Eq. 1). In Eq. (3), g_J is the gyromagnetic ratio of the electron, and g_I' is that of the nucleus, both in units of the Bohr magneton μ_0 . (We can also write $g_I' = g_I \mu_N / \mu_0$, where μ_N is the nuclear

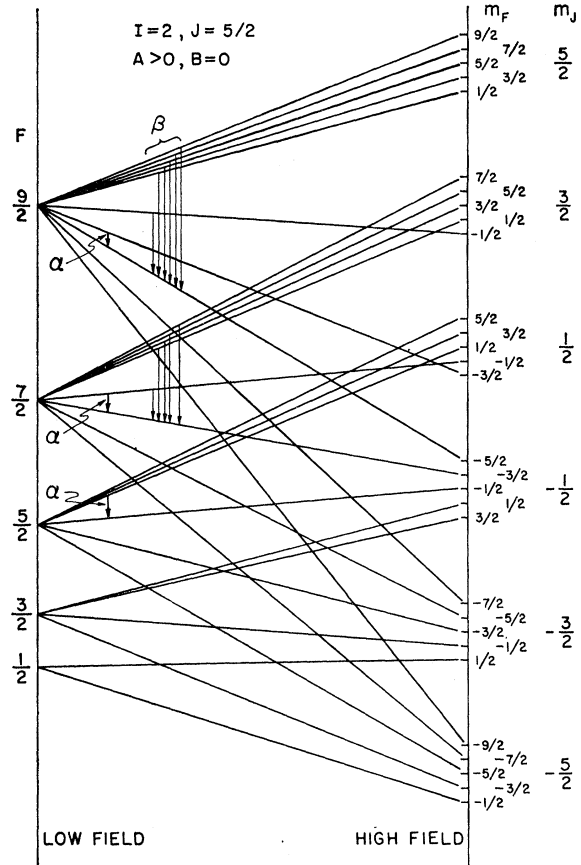


FIG. 1. Schematic diagram of the behavior of the hyperfine magnetic sublevels as a function of applied external magnetic field, for $I=2$, $J=5/2$. The drawing is not to scale, and is intended to show only the general ordering of the levels. α and β label possible transitions detectable in the atomic beam apparatus.

magneton.) The sign convention is such that the gyromagnetic ratio is positive for the electron.

At low fields, the $(IJFM_F)$ representation gives the approximate eigenstates of the Hamiltonian [Eq. (1) plus Eq. (3)]; at high fields, however, Eq. (3) dominates the total Hamiltonian, and the $(IJm_I m_J)$ representation gives the eigenfunctions. Schematically, the dependence of the splitting on H_E can be seen by connecting low- and high-field values of the energies, as in Fig. 1 (drawn for $I=2$, $J=5/2$, the values appropriate to Sc^{44}). The actual field dependence of the levels is not linear, of course, and must be obtained by either perturbation approximations, or, more exactly, by computer diagonalization of the total Hamiltonian.

As indicated above, the measurements are made by inducing transitions between the magnetic sublevels of the hfs. Because of the trajectories of the atoms in passing through the magnets of the apparatus, the only detectable transitions are those in which the atom in its initial state has a negative effective magnetic moment ($\mu_{\text{eff}} = -\partial E / \partial H$) at very high values of H_E , and in which the final state has positive μ_{eff} at the same H_E .

This selection of detectable transitions is made by the strong inhomogeneous fields in the first and last magnets of the apparatus. The actual transitions are induced in the central magnet, at low values of H_E , and were limited in these experiments to $\Delta F=0$ transitions. For such transitions the dipole selection rules require $\Delta M_F = \pm 1$, and normally only the transitions α would be observed. If sufficient power is supplied to the rf loop used to induce the transitions, multiple-quantum absorption is possible and transitions such as β will be seen. The frequencies at which such transitions will take place will be $1/N$ times the total frequency separation of the initial and final states, when N is the number of quanta absorbed. These quantities can be calculated by

applying perturbation theory to the total Hamiltonian; to second order in H_E , the frequency for the transition by N quantum absorption may be written as⁴

$$\nu(N) = g_F \left(\frac{\mu_0 H_E}{h} \right) + \left[\frac{P}{\Delta\nu_{F+1,F}} - \frac{Q}{\Delta\nu_{F,F-1}} \right] \times [N + 2m_F(\text{final})] \left(g_J \frac{\mu_0 H_E}{h} \right)^2 + \dots \quad (4)$$

In this equation, m_F (final) is the total magnetic quantum number of the final state, and the other quantities are defined by the relations

$$P = \frac{(F+1-J+I)(F+1+J-I)(F+I+J+2)(J+1-F)}{4(F+1)^2(2F+1)(2F+3)},$$

$$Q = \frac{(F-J+1)(F+J-I)(J+I+F+1)(J+I-F+1)}{4F^2(2F-1)(2F+1)},$$

$$N = \text{quantum multiplicity} = m_F(\text{initial}) - m_F(\text{final}), \quad (5)$$

$$g_F = g_J \frac{F(F+1) - I(I+1) + J(J+1)}{2F(F+1)} + g_I' \frac{F(F+1) + I(I+1) - J(J+1)}{2F(F+1)},$$

$$\Delta\nu_{F,F-1} = \frac{E_F - E_{F-1}}{h},$$

and E_F and E_{F-1} are the appropriate eigenvalues of Eq. (1). Equation (4) contains a further approximation in that the explicit dependence on g_I' of the term quadratic in H_E has been dropped.

The frequency spectrum expected from the quadratic approximation [Eq. (4)] at a given value of H_E is a comb of equally spaced resonance peaks, the spacing between which depends on the $\Delta\nu$'s, and, hence, on A and B of Eq. (2). The resonance peaks themselves are composed of several transitions, all of which take place at the same frequency; the degeneracy arises because $N + 2m_F$ (final) may be the same for different values of N and m_F (final). The detailed composition of the resonances expected in the Sc^{44} are shown in Fig. 2, where the possible transitions are plotted with an arbitrary splitting according to their values of $N + 2m_F$ (final), for both $I=2$ and $I=6$, with $J=\frac{5}{2}$, and $F=\frac{9}{2}$, and $F=17/2$, respectively.

The extent to which each of the individual transitions shown in Fig. 2 contributes to the observed height of the corresponding resonance depends on the rf power supplied to the loop. Most of the resonances in the comb have three contributing transitions, corresponding to quantum multiplicities N , $N+2$, and $N+4$. The probability of inducing an observable transition is a function of the quantum multiplicity, and each transition contributing to a given resonance will have optimum

transition probability at a different value of rf power. Hence, it is not obvious what choice of power will optimize the observed signal. A complete discussion of this problem is given by Christensen *et al.*,⁴ and will not be treated here. The best results in the present case were achieved by operating at the power which optimized the transition probability for the highest multiple-quantum transition in a resonance.

Hfs of the $I=2$ State

Hyperfine structure separations were determined for $I=2$ in the ${}^2D_{5/2}$ electronic state, between the $F=\frac{9}{2}$, $F=\frac{7}{2}$, and $F=\frac{5}{2}$ levels. The ${}^2D_{5/2}$ state of scandium is not the ground state, but was thermally populated in the oven, and is favored over the ${}^2D_{3/2}$ ground state by our machine optics because of its greater effective moment in high m_J states. The separations were determined by following resonances in the $F=\frac{9}{2}$ and $F=\frac{7}{2}$ levels as a function of H_E up to the fields at which the third-order terms in Eq. (4) began to contribute. This occurred at about 22 G, corresponding to a potassium transition frequency of about 17 Mc/sec. At the highest values of H_E , the multiple-quantum peaks discussed in Sec. I were well resolved, as seen in Fig. 3. Five multiple-quantum peaks were observed in the $F=\frac{9}{2}$ level studies, and three in the $F=\frac{7}{2}$ level; in each case the resonance of lowest frequency has a linear field dependence, cor-

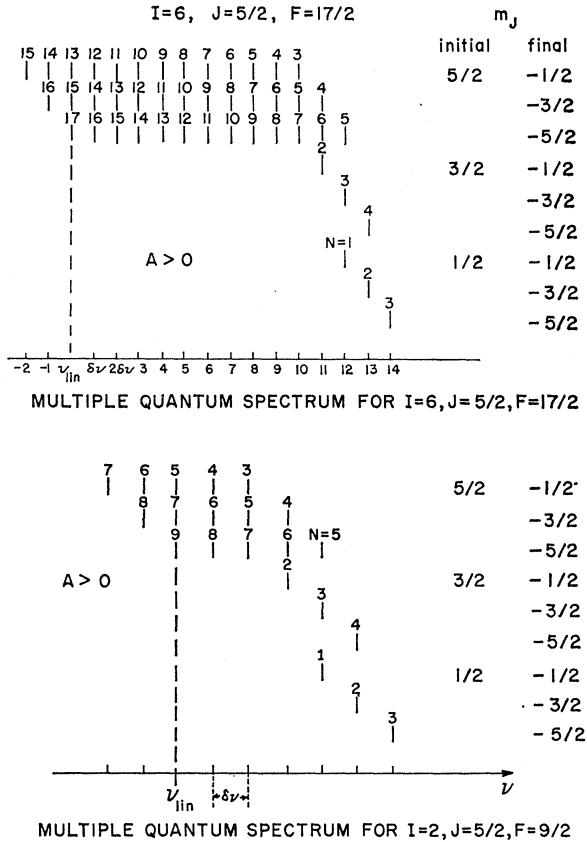


FIG. 2. A schematic diagram of the expected frequencies of the transitions detectable in the apparatus. The individual transitions are labelled by their quantum multiplicity, and arranged in the figure according to their initial and final state values of m_J . The figures are plotted for $A > 0$; taking the opposite sign for A does not change the character of the pattern. The frequency degeneracy of the several transitions is valid only in the quadratic approximation for the external-field dependence.

responding to $N + 2m_F = 0$ in the second term of Eq. (4). The data in Fig. 3 do not cover the region of the third resonance in the comb; this resonance was seen at lower fields, but was not checked here, since little additional accuracy in the overall experiment would result.

The observation of the resonance with linear dependence on H_E has obvious advantages. In the first place, it serves as a reference point for the quadratic splitting of the other resonances, and, hence, makes possible a measurement of the $\Delta\nu$ which is independent of assumptions about the g_J of the atom. In the second place, its dependence on H_E is a direct measurement of g_F in Eq. (4), and hence, if g_I is known, measures directly the g_J . In these experiments the magnitude of g_I was known from the quadratic splitting, but not the sign. Ignoring the contribution of g_I to the g_F term in Eq. (4), the measurements gave the value $g_{5/2} = 1.202 \pm 0.004$; including the g_I term, gave the results:

$$\begin{aligned} g_{5/2} &= 1.2008 \pm 0.0003 & \text{if } \mu_I > 0 \\ &= 1.1997 \pm 0.0003 & \text{if } \mu_I < 0. \end{aligned} \quad (6)$$

The values for g_I were obtained from the second term in Eq. (4), and the data in Fig. 3. Small corrections for third-order terms were made, with the results

$$\Delta\nu_{9/2, 7/2} = 477 \pm 11 \text{ Mc/sec},$$

$$\Delta\nu_{7/2, 5/2} = 355 \pm 5 \text{ Mc/sec}.$$

From these $\Delta\nu$'s, the hyperfine coupling constants A and B were computed to be

$$|A(^2D_{5/2})| = 102.6 \pm 1.2 \text{ Mc/sec},$$

$$|B(^2D_{5/2})| = 22.9 \pm 14.0 \text{ Mc/sec},$$

$$\text{with } B/A > 0.$$

This, coupled with measurements of Sc^{45} (where μ , Q , A , and B are all known independently) may be used with the Fermi-Segrè formula (assuming no hfs anomaly) to determine μ and Q , giving

$$|\mu(I=2)| = 2.56 \pm 0.03 \text{ nm},$$

$$|Q(I=2)| = (0.14 \pm 0.08) \times 10^{-24} \text{ cm}^2,$$

$$\text{with } \mu/Q > 0.$$

Hfs of the $I=6$ State

The hyperfine structure of the $I=6$ state is somewhat more complicated than that for $I=2$. The high value of the nuclear spin increases the multiplicity of the levels, and so the number of resonances in the multiple-quantum comb correspondingly increases. The expected transition pattern is shown in Fig. 2. In contrast to the $I=2$ data, we could no longer directly observe the resonance at the linear frequency. We did observe seven resonances in the comb, corresponding to the same orders of quantum multiplicity as in the $I=2$ work. The resonance pattern for the highest value of H_E in the $F=17/2$ state is shown in Fig. 4. Similar results were obtained for the $F=15/2$ level.

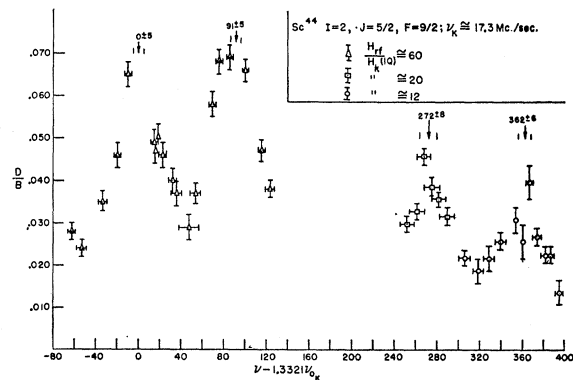


FIG. 3. Experimental results for Sc^{44} for the parameters $I=2$, $J=5/2$, $F=9/2$ at a magnetic field corresponding to a potassium frequency $\nu_k \approx 17.3 \text{ Mc/sec}$. D/B is the ratio of the "flopped" beam to the transmitted beam. The frequency scale is chosen so that the zero frequency corresponds to the linear frequency for scandium.

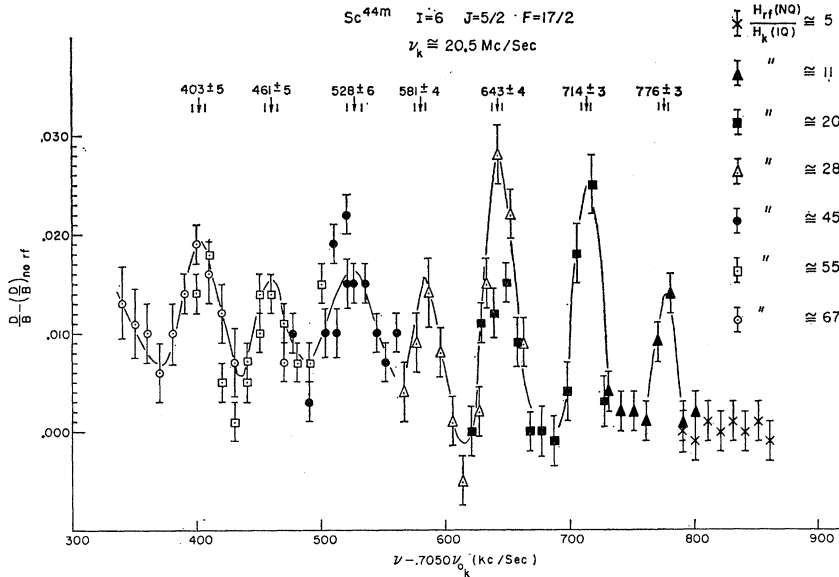


FIG. 4. Experimental results for Sc^{44} for the parameters $I=6$, $J=\frac{5}{2}$, $F=17/2$, at a magnetic field corresponding to a potassium frequency $\nu_k \approx 20.5$ Mc/sec. D/B is the ratio of the "flopped" beam to the transmitted beam. The frequency scale is chosen so that the zero frequency corresponds to the linear frequency for scandium.

The assignment of the proper value of $N+2m_F$ (final) to the observed resonances was accomplished in the following way: First, the value of the linear frequency [$N+2m_F$ (final)=0] was inferred from the g_J data for the $I=2$ state. The observed resonances were then assigned their most plausible values of [$N+2m_F$ (final)], consistent both with the separation between resonances and with their inferred splitting from the linear frequency. Only one choice of [$N+2m_F$ (final)] assignments proved to be consistent with all the data, but this choice did not distinguish between the two values for g_J given in Eq. (6).

The rest of the analysis was essentially the same as for the $I=2$ case. The results were

$$\begin{aligned} |A(^2D_{5/2})| &= 53 \pm 2 \text{ Mc/sec}, \\ |B(^2D_{5/2})| &= 62 \pm 50 \text{ Mc/sec}, \end{aligned} \quad (7)$$

with $B/A < 0$.

These gave the following values for the moments:

$$\begin{aligned} |\mu(I=6)| &= 3.96 \pm 0.15 \text{ nm}, \\ |Q(I=6)| &= (0.37 \pm 0.29) \times 10^{-24} \text{ cm}^2, \end{aligned} \quad (8)$$

with $\mu/Q < 0$.

IV. DISCUSSION

As stated briefly in the introduction, one reason for measuring the magnetic moments of Sc^{44} is to check the extent of the agreement with a simple odd-group model prediction in the odd-odd nuclei in the $f_{7/2}$ shell. The central assumption of such a model is that I_p and I_n , the total proton and neutron angular momenta, are good quantum numbers, with the total angular momentum I their vector sum. This model has been quite successful in nuclei where neutrons and protons are filling different shells. In the $f_{7/2}$ shell, however, I_p and

I_n are almost certainly not good quantum numbers, because of the possible strong neutron-proton interactions.

It is surprising, therefore, that in Mn^{52} the measured moments agree very well with the odd-group model predictions. Mn^{52} is a nucleus directly comparable to Sc^{44} ; it has one neutron hole and three proton holes in the $f_{7/2}$ shell, as opposed to the one proton and three neutrons of Sc^{44} . The odd-group model prediction for magnetic moments is given by

$$\frac{\mu_I}{I} = \frac{1}{2}(g_p + g_n) + \frac{1}{2}(g_p - g_n) \left(\frac{I_p(I_p+1) - I_n(I_n+1)}{I(I+1)} \right), \quad (9)$$

and using Schmidt values for the gyromagnetic ratios g_p and g_n and putting $I_p = I_n = \frac{7}{2}$, the states in Mn^{52} fit almost exactly (see Table I). The same values are expected within the model for the states in Sc^{44} . Here the fit is not as good, and for the $I=2$ is especially poor.

TABLE I. Comparison of magnetic moments of Mn^{52} and Sc^{44} . The first two rows give the experimental results; the third, the simple odd-group model predictions. A test of the consistency of general $(f_{7/2})^4$ wave functions is provided by the fourth and fifth rows (see text).

	$\mu_I/I, I=2$	$\mu_I/I, I=6$
$^{25}\text{Mn}_{27}^{52}$	0.52 ± 0.08^a	0.53 ± 0.08^a
$^{21}\text{Sc}_{23}^{44}$	1.28 ± 0.02	0.66 ± 0.03
Odd-group model prediction	0.55	0.55
($I_p = I_n = \frac{7}{2}$)		
Sum of $\text{Sc}^{44} + \text{Mn}^{52}$	1.80 ± 0.04	1.19 ± 0.04
$g_p + g_n$ (Schmidt)	1.11	1.11

^a See Ref. 2.

The Sc^{44} $I=2$ state moment can be fit, of course, by assuming that I_n is not a good quantum number. One can take linear combinations of states defined by I_p and different values of I_n , and with such wave functions fit a wide range of data. This procedure is an extension of the model and does not give unique answers. However, any wave function of the four $f_{7/2}$ particles can be written in this way, since the odd-group model states form a complete orthogonal set. The magnetic moments predicted for such linear combinations will all have the form

$$\frac{\mu}{I} = \frac{(g_p + g_n)}{2} + \beta \frac{(g_p - g_n)}{2}, \quad (10)$$

since the first term in Eq. (9) does not depend on I_p or I_n . The constant β in Eq. (10) will depend on the particular linear combination of odd-group model wave functions employed.

One can correlate the magnetic moments of Sc^{44} and Mn^{52} by using Eq. (10). Since the nuclei are particle-hole conjugates of each other, they should have the same eigenfunctions for analogous states, except that the role played by neutrons and protons will be interchanged. Hence, whatever β may be for a given state in Sc^{44} , the analogous state in Mn^{52} should have the same β . The sign of the second term in Eq. (10) will be different for the different nuclei, however, because of the replacement of protons by neutrons (holes) and neutrons by proton (holes). The absolute magnitude of the magnetic moments will still be ambiguous, because of the indefiniteness of β , but the sum of the moments of analogous states in the two nuclei will be

$$\frac{\mu_I(\text{Sc}^{44})}{I} + \frac{\mu_I(\text{Mn}^{52})}{I} = g_I(\text{Sc}^{44}) + g_I(\text{Mn}^{52}) = g_p + g_n. \quad (11)$$

The comparison of these sums with Schmidt values of $g_p + g_n$ is also given in Table I. Note that for the $I=6$ states the agreement is excellent, while for the $I=2$ states it is poor.

The argument leading to Eq. (11) assumes that the proper analog states have been identified in the $(f_{7/2})^4$ configurations, and nothing further. The $I=2$ states are, therefore, apparently not analogs in this sense. This result is not surprising; if the analogy were good, not only would Eq. (11) be valid, but the spectra of the two isotopes would be identical. But since the $I=6$ states are such good analogs, it would not be surprising if both states in one of the two isotopes were well described by $(f_{7/2})^4$ wave functions. Whether Mn^{52} or Sc^{44} is better described in these terms cannot be determined from the

magnetic moments alone, however. Both moments in either nucleus can be fit by a $(f_{7/2})^4$ wave function, as is apparent from Eq. (9). In the absence of energy eigenfunctions, one must assume a given coupling of the four particles to make any calculation at all.

Efforts have been made in the past to construct wave functions which may also be energy eigenfunctions, to see if an agreement with magnetic moments in this region could be reached. The most recent of these attempts is due to Lawson,⁸ and achieves good general agreement over the shell. His method of construction is closely analogous to the Nilsson model for odd-even nuclei. In the present instance he predicts the $I=2$ state magnetic moment for the $(f_{7/2})^4$ configuration to be $\mu = +2.56 \text{ nm}$.⁹ This value is remarkably close to the Sc^{44} value.

An alternate construction of states is the seniority classification of Flowers,¹⁰ which categorizes the states according to their angular momentum I , isotopic spin T , and seniority v . The magnetic moments for these states can be uniquely specified only in those cases where this classification is sufficient to completely specify the states. In the four-particle case above, there are three states of angular momentum 2, one with seniority 2, and two with seniority 4. For the seniority-2 states, the magnetic moment can be calculated. Using a method to be described in a future paper, these moments can be shown to be

$$I=2: \mu_I = 0.56 \text{ nm};$$

$$I=6: \mu_I = 1.67 \text{ nm}.$$

These fit neither the Mn^{52} nor the Sc^{44} moments, and thus seem to indicate that seniority is probably not a good quantum number. The observed states could, of course, be pure $v=4$ states; in such a case, the states cannot be uniquely specified without further assumptions about the wave functions.

ACKNOWLEDGMENTS

We gratefully acknowledge the advice and aid of Professor D. R. Hamilton throughout this investigation. We wish to thank Dr. B. F. Bayman and Dr. I. Talmi for many fruitful discussions on the theoretical interpretation. Our thanks also to Dr. R. D. Lawson for communicating his unpublished results, and to Dr. J. J. Pinajian of Oak Ridge National Laboratory for his cooperation in obtaining sources.

⁸ R. D. Lawson, Phys. Rev. **124**, 1500 (1961).

⁹ R. D. Lawson (private communication).

¹⁰ B. H. Flowers, Proc. Roy. Soc. (London) **212**, 248 (1952).